NOTES AND CORRESPONDENCE

Nitric Acid–Sea Salt Reactions: Implications for Nitrogen Deposition to Water Surfaces

S. C. PRYOR

Atmospheric Science Program, Department of Geography, Indiana University, Bloomington, Indiana

L. L. SØRENSEN

Department of Wind Energy and Atmospheric Physics, Risø National Laboratory, Roskilde, Denmark

23 August 1999 and 20 October 1999

ABSTRACT

Many previous studies have indicated the importance of nitric acid (HNO_3) reactions on sea salt particles for flux divergence of HNO_3 in the marine surface layer. The potential importance of this reaction in determining the spatial and temporal patterns of nitrogen dry deposition to marine ecosystems is investigated using models of sea spray generation and particle- and gas-phase dry deposition. Under horizontally homogeneous conditions with near-neutral stability and for wind speeds between 3.5 and 10 m s^{-1}, transfer of HNO_3 to the particle phase to form sodium nitrate may decrease the deposition velocity of nitrogen by over 50%, leading to greater horizontal transport prior to deposition to the sea surface. Conversely, for wind speeds above 10 m s^{-1}, transfer of nitrogen to the particle phase would increase the deposition rate and hence decrease horizontal transport prior to surface removal.

1. Introduction

a. Nitrogen deposition to aquatic ecosystems

Most oceanic primary production by phytoplankton is limited by nutrient availability. The limiting nutrients commonly are nitrogen (N) and phosphorous (P). Increasing N and P concentrations have profound implications for ecosystem health and productivity. For example, Paerl (1995) suggests ''nitrogen-limited estuaries, shallow coastal and continental shelf waters account for nearly half the global oceanic primary production.'' Typically, absorption of nitrate (NO_3^-), nitrite (NO_2^-), and ammonium (NH_4^+) from ocean waters supplies N required by organisms. Human activity has increased the concentration of these and other N compounds in coastal waters, leading in some cases to greatly enhanced primary production or eutrophication (Paerl 1995). A number of studies indicate that between 10% and more than 50% of coastal N loading is attributable to atmospheric fluxes (e.g., Paerl 1995; Rendell et al. 1993). Although the contribution of wet and dry deposition and gas- and particle-phase N to this atmospheric flux is uncertain and highly variable spatially, Paerl (1995) summarizes data that suggest dry deposition is a significant contributor to the atmospheric flux to all of the major oceans (i.e., dry deposition is greater than 20% of the total flux), and model calculations for the seas around Denmark indicate that one-third of the total N comes from the atmosphere and approximately three-fifths of the atmospheric deposition (via wet and dry pathways) comes from particulate matter (Asman et al. 1995). It also has been suggested that atmospheric fluxes to midlatitude coastal areas may be largest in the late spring and summer months, when nutrient concentrations are generally at a minimum and hence the effect of this flux may be disproportionately large (Fisher and Oppenheimer 1991; Rendell et al. 1993).

Nitrogen deposition is determined largely by emissions of the following N-containing gases: nitric oxide (NO), nitrogen dioxide (NO_2), ammonia (NH_3), and nitrous oxide (N_2O). Nitric acid (HNO_3) is formed principally as a result of NO and NO_2 and has been shown to make a significant contribution to total N deposition in a number of diverse terrestrial and marine environments [e.g., in the studies of Sievering et al. (1992), Pryor et al. (1999b), and Asman et al. (1995), HNO_3 deposition contributed approximately 10% of the total N flux].

Nitrogen emissions to the atmosphere are currently twice ''natural background'' levels (Vitousek et al.

Corresponding author address: S. C. Pryor, Atmospheric Science Program, Dept. of Geography, Indiana University, Bloomington, IN 47405.
E-mail: spryor@indiana.edu

1997) and are predicted to increase by 25%–50% in less-developed regions by 2020 (Galloway et al. 1994). These projections indicate the importance of improved understanding of atmosphere–surface exchange and the potential for an enhanced role of atmospheric deposition in eutrophication problems in the twenty-first century.

b. Dry deposition processes

Because of difficulties in direct measurement of dry deposition fluxes of particles and some gases, dry deposition often is determined by the ''concentration method'' in which the flux F is given by multiplication of the concentration at some level above the surface by a deposition velocity:

$$F = -v_d(z)[C(z) - C(0)], \quad (1)$$

where $C(z)$ is concentration at measurement height z; $C(0)$ is concentration at the surface (which may be zero depending on surface uptake); $v_d(z)$ = deposition velocity, which may be computed as the inverse of the sum of a number of resistances plus a gravitational settling term for particles:

$$v_d = \frac{1}{r_a + r_b + r_c} + v_g. \quad (2)$$

In Eq. (2) the following are true.

1) r_a is aerodynamic resistance. This term represents the resistance to transport by turbulence to the quasi-laminar surface layer.
2) r_b is quasi-laminar surface layer resistance. Very close to the surface, a laminar boundary layer forms (depth $\approx$ 100–1000 μm), which essentially is free of turbulence. Transport across this layer is largely the result of Brownian diffusion.
3) r_c is surface resistance. For highly reactive or soluble gases the surface resistance is small. We assume a surface resistance of zero and 100% efficient surface capture for particle deposition to water surfaces.
4) v_g is gravitational settling velocity. For coarse-mode particles, the downward gravitational force exceeds the drag force from the viscosity of air, and hence v_g is important. This transport process is negligible for gases and fine particles, however.

Additional processes that may be of importance to particle dry deposition but are not considered here include interception and inertial forces, electrical migration due to surface charge, and thermophoresis caused by temperature gradients (see Zufall and Davidson 1998).

c. The focus of this note

The majority of studies of dry deposition fluxes to surfaces explicitly or implicitly rely upon the constant flux layer assumption (i.e., that the measured or determined flux at a given height above the surface is equal to the flux at the surface). Flux divergence (i.e., violation of this assumption), however, may occur because of advection, storage effects, or chemical reactions between the measurement height and the ground (Kramm and Dlugi 1994). Reaction of HNO_3 on sea salt (NaCl) particles to yield sodium nitrate ($NaNO_3$) in the particle phase and volatize hydrochloric acid vapor (HCl) is a potentially important source of flux divergence of HNO_3 over the sea surface (Geernaert et al. 1998). This chemical reaction and others on and in sea salt aerosols also have been shown to play critical roles in halogen (particularly chlorine and bromine) release in the marine boundary layer (Sander and Crutzen 1996), which has been linked to ozone depletion [e.g., the rapid decrease in ozone concentrations in Arctic air masses during the spring (Barrie et al. 1988)].

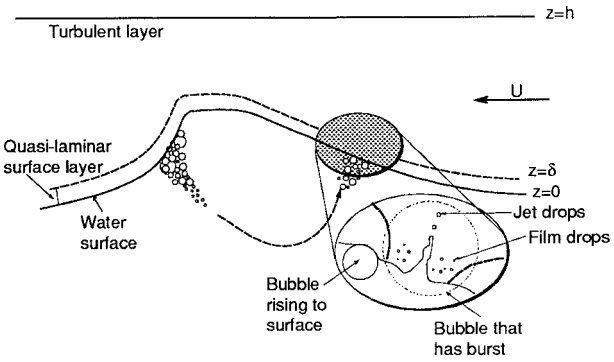

FIG. 1. A schematic of the particle deposition model, illustrating that the model is composed of two layers, a well-mixed turbulent layer in which gravitational settling and turbulent transport are responsible for the transfer of particles toward the surface, and the quasi-laminar surface layer in which gravitational settling of ''wet'' particles and diffusional transport are the primary transport mechanisms. This figure is adapted from Hummelshøj et al. (1992).

In this note, the reaction of HNO_3 on sea salt is considered from a different perspective. The rate constant for the HNO_3–NaCl reaction is thought to be rapid (Fenter et al. 1994), and the reaction has a large equilibrium constant (Seinfeld and Pandis 1998), so, given sufficient particle surface area (and time), the reaction is expected to reach completion with near total transfer of N to the particle phase. Here a first analysis of the potential role of this reaction in modifying atmosphere–surface fluxes of N is presented. It is demonstrated that this transfer of N from the gas to the particle phase has the potential to modify substantially the spatial and temporal patterns of the flux of N to the sea surface.

2. Modeling particle dry deposition to water surfaces

a. Description of the model

Here the model of particle dry deposition velocity described by Pryor et al. (1999) and based on work by Williams (1982) and Hummelshøj et al. (1992) is used.

A schematic of the model is shown in Fig. 1. The form of the model is

$$v_d = \frac{(v_h + v_{g,d})(v_\delta + v_{g,w})}{v_h + v_\delta + v_{g,d}}, \quad (3)$$

where v_h is transfer velocity in the layer dominated by turbulent transfer, $v_{g,d}$ and $v_{g,w}$ are gravitational settling transfer velocities (subscripts d and w indicate dry and wet particles, respectively, where dry particles are those present in the marine atmosphere above the quasi-laminar surface layer, and wet particles refer to particles that have taken up water as they approach the surface and are subject to higher humidities), and v_δ is transfer velocity across laminar surface layer. These terms are given by the following equations.

1) Transfer velocity due to turbulent processes:

$$v_h = \frac{1}{\frac{1}{\kappa u_*}\left[\ln\left(\frac{z_r}{z_{0m}}\right) - \Psi_h\left(\frac{z_r}{L}\right) + \Psi_h\left(\frac{z_{0m}}{L}\right)\right]}, \quad (4)$$

where κ is the von Kármán constant, u_* is friction velocity, z_r is reference height, z_{0m} is momentum roughness length, Ψ_h is the stability correction, and L is Monin–Obukhov length.

2) Transfer velocity due to gravitational settling:

$$v_{g,x} = \left[\frac{g}{18\mu}\left(\frac{\rho_p}{\rho_{\text{air}}}\right)d_x^2\right]C, \quad (5)$$

where g is gravity, μ is dynamic viscosity, ρ_p is particle density, ρ_{air} is air density, d_x is particle diameter ($x = d$ or w), and C is the Cunningham slip correction factor $\{C = 1 + (\lambda/d)[2.514 + 0.8\exp(-0.55d/\lambda)]$; λ is the mean free path of air; Seinfeld and Pandis 1998$\}$. For $v_{g,w}$, d is adjusted for hygroscopic growth in the quasi-laminar surface layer [i.e., $x = w$, so $d = d_w$, where d_w is dependent on relative humidity ($\leq$98.3% over salt water) and particle composition using the approximations of Fitzgerald (1975)].

3) Transfer velocity across the quasi-laminar surface layer:

$$v_\delta = (1 - \alpha_{\text{bob}})(cu_*\text{Sc}^{-0.5}\text{Re}^{-0.5} + u_* \times 10^{-3/\text{St}}) + \alpha_{\text{bob}}\left[\frac{u_*}{U_{10}} + \text{Eff}(2\pi r_{\text{drop}}^2)(2z_{\text{drop}})\frac{q_{\text{drop}}}{\alpha}\right], \quad (6)$$

where α_{bob} is relative area with bursting bubbles, $c = 1/(c_1\sqrt{c_2})$, $c_1 = f$(thickness of the molecular diffusion layer), $c_2 = f$(ratio of the height of roughness elements to the aerodynamic roughness length), Sc is Schmidt number [Sc $= \nu/D$, where ν is the kinematic viscosity of air, diffusivity $D = kTC/(3\pi\mu d)$, k is the Boltzmann constant, and T is temperature], Re is Reynolds number (Re $= u_* z_{0m}/\nu$), St is Stokes number [St $= u_*^2 v_{g,x}/(\nu g)$], U_{10} is wind speed at 10 m, Eff is the effectiveness with which particles are collected by the spray drops, z_{drop} is the average height that spray drops reach, r_{drop} is the average radius of spray drops, q_{drop} is the flux of spray drops from the surface, and α is the area of sea surface covered by whitecaps:

$$\alpha = 1.7 \times 10^{-6}\, U_{10}^{3.75}, \quad (7)$$

from Wu (1988).

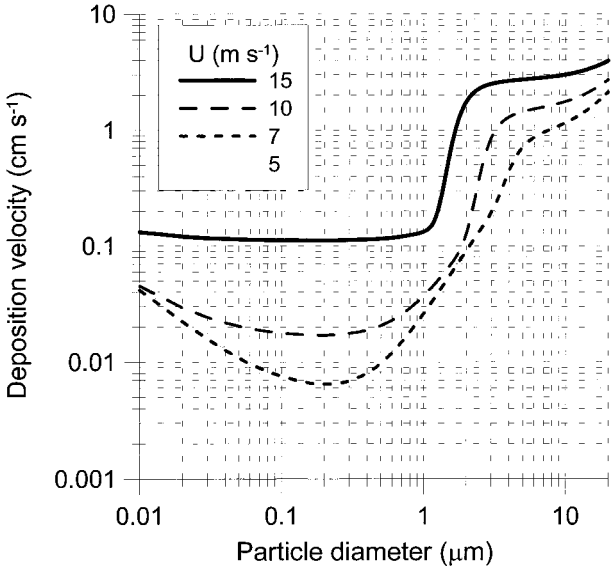

FIG. 2. Modeled particle v_d as a function of wind speed and particle diameter for NaCl particles. Note that u_* and z_{0m} for the specified U_{10} are obtained by iterative solution of the logarithmic wind profile and Charnock formula (the Charnock constant is assumed to have a value of 0.0185).

Transfer across the quasi-laminar surface layer represents the major limitation on fine particle deposition. The two components of (6) pertain to diffusional transfer through the quasi-laminar surface layer (also referred to as the viscous sublayer) and to the increase in downward movement of particles due to bubble burst activity [see discussion in Pryor and Barthelmie (2000)].

Deposition velocities computed using this model are shown in Fig. 2 for pure NaCl particles and near-neutral atmospheric stratification for four different wind speeds. The characteristic form of the graph with lowest deposition velocity for particles with $d \approx 0.1$–0.4 μm reflects higher deposition velocity for larger particles for which gravitational settling is nonnegligible and for smaller particles for which Brownian diffusion is more efficient. This figure also emphasizes the importance of wind speed in determining deposition velocity (e.g., as U_{10} increases from 5 to 15 m s^{-1}, v_d for $d = 0.2$ μm increases more than fortyfold). As wind speeds increase, the size dependence of deposition velocity for particles below 1 μm decreases as enhancement of deposition due to bubble burst activity increases, and so the limitation placed on deposition by particle diffusivity is effectively removed.

TABLE 1. Comparison of model performance and observations of particle dry deposition to water surfaces.

	z_0 (m)	u_* (m s^{-1})	Particle description	Observed v_d (cm s^{-1})	Modeled v_d (cm s^{-1}) without bubbles	Modeled v_d (cm s^{-1}) with bubbles
Sehmel and Sutter (1974) cited in Slinn et al. (1978)	2×10^{-5}	0.11	$d = 2.5$ μm $\rho = 1.5$ g cm^{-3}	6.0×10^{-3} 1.2×10^{-2}	3.2×10^{-2}	4.6×10^{-2}[a]
	2×10^{-5}	0.11	$d = 1.0$ μm $\rho = 1.5$ g cm^{-3}	2.0×10^{-2}	8.7×10^{-3}	1.1×10^{-2}[a]
	2×10^{-4}	0.44	$d = 7.0$ μm $\rho = 1.5$ g cm^{-3}	2.0, 4.5	1.5	1.5[a]
	2×10^{-4}	0.44	$d = 3.0$ μm $\rho = 1.5$ g cm^{-3}	1.0×10^{-1}	4.5×10^{-2}	1.0×10^{-1}[a]
Moller and Shumann (1970) cited in Slinn et al. (1978)	$\approx 5 \times 10^{-4}$	≈ 0.4	$d = 0.03$ μm NaCl	4.0×10^{-2}	1.0×10^{-2}	3.4×10^{-2}[a]
Larsen et al. (1995)	Not specified[c] $U = 3$ m s^{-1}		$d = 0.2$ μm MgO	No bubbles: 3.4×10^{-2} Bubbles: $\pm 30\%$[b]	2.8×10^{-2}	4.6×10^{-2}
	Not specified[c] $U = 6$ m s^{-1}		$d = 0.2$ μm MgO	No bubbles: 6.4×10^{-2} Bubbles: $\pm 30\%$[b]	5.6×10^{-2}	1.1×10^{-1}
	Not specified[c] $U = 9$ m s^{-1}		$d = 0.2$ μm MgO	No bubbles: 1.2×10^{-1} Bubbles: $\pm 30\%$[b]	9.5×10^{-2}	1.8×10^{-1}

[a] Here U_{10} is inferred from the logarithmic wind profile and observed z_0 and u_*, α was calculated based on U_{10}.
[b] Bubble burst simulated with bubblers. Bubblers set to give alpha = 0.08 (representative of a wind speed of 17 m s^{-1}).
[c] z_0 calculated from the Charnock formula and u_* from the logarithmic wind profile.

b. Evaluation of the model

Only a few direct measurements of particle dry deposition to water surfaces are available in the literature for evaluation of mathematical models of deposition velocities, and the majority derive from wind-tunnel experiments (Slinn et al. 1978; Larsen et al. 1995; Zufall and Davidson 1998). Table 1 summarizes a comparison of the model performance relative to three wind-tunnel experiments for a range of particle and environmental parameters. As shown, the model performs well relative to the measurements, particularly in light of the experimental error and uncertainties in initializing the model. The model is within a factor of 2 for all comparisons except the experiment reported in Slinn et al. (1978) for a particle diameter of 2.5 μm. For this experiment the model underestimates observations, but this underestimate may be caused by the model assumption that the particles are hydrophobic (the particle composition is not specified in the experimental description). If only 10% of the particles were ammonium nitrate (NH_4NO_3) (or another hydroscopic compound) the model would predict the deposition velocity correctly.

3. The role of particles in modifying gas fluxes: HNO_3–sea salt interactions

To illustrate the potential importance of HNO_3–sea salt reactions on the spatial and temporal patterns of N fluxes to water surfaces, it is useful to compare the deposition velocity for HNO_3 in the absence of reactions with sea spray with the deposition velocity for the particles that might act as the sink for HNO_3 (via formation of $NaNO_3$). To make this comparison, some simplifying assumptions are made about the uptake of HNO_3 on sea salt and the prevailing atmospheric conditions. With respect to the prevailing meteorological conditions, we assume near-neutral stability and horizontal homogeneity. We also assume that, since reaction of HNO_3 with NaCl particles is a surface reaction (Mamane and Gottlieb 1992; Fenter et al. 1994), the size distribution of the resulting $NaNO_3$ can be characterized by particle diameters associated with the maximum surface area of NaCl particles.

To calculate the surface-area size distribution for sea spray droplets, the following equations developed by Monahan et al. (1986) to describe spray generation in open ocean conditions are used. The generation of sea salt droplets per unit area of sea surface [by bubble burst (F_0) and spume (F_1)], per increment of droplet radius r per second is given by

$$\frac{dF_0}{dr} = 2.373U_{10}^{3.41}r^{-3}(1 + 0.057r^{1.05}) \times 10^{1.19e^{-B^2}}, \quad (8)$$

$$B = \frac{0.380 - \log r}{0.65}, \quad (9)$$

and spume ($r > 10$ μm):

$$\frac{dF_1}{dr} = 8.6 \times 10^{-6}e^{2.08U_{10}}r^{-8}, \quad (10)$$

where F is the flux due to bubble burst (subscript 0) or spume (subscript 1). Note that (10) is known to overestimate the flux of large droplets, but this overestimation does not affect the analysis because the surface area of sea spray is dominated by r less than 10 μm (Smith et al. 1993).

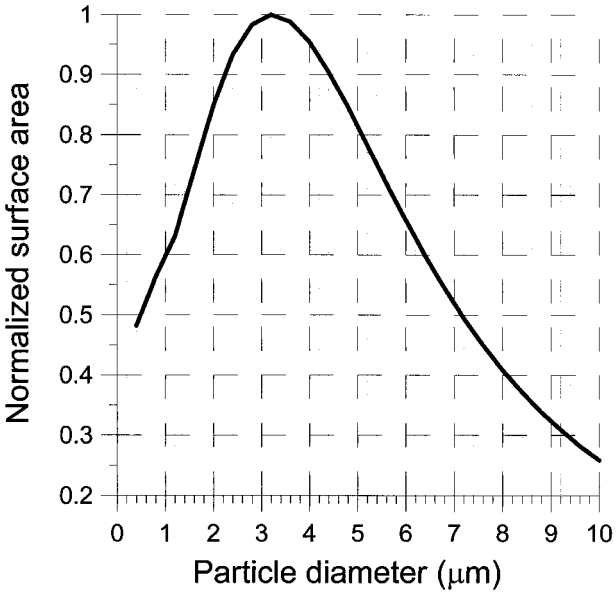

FIG. 3. The normalized surface area of NaCl droplets computed using (8)–(10). For clarity only data for $r \leq 10$ μm are shown here.

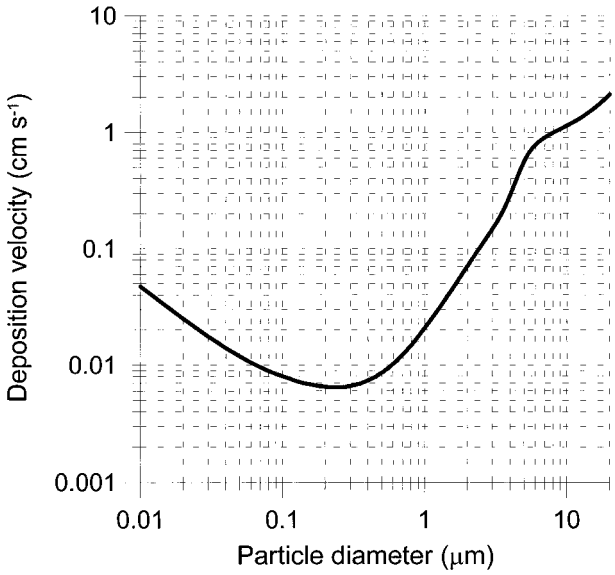

FIG. 4. Modeled particle v_d for an $NaNO_3$ particle spectrum presented as a function of particle d. Here, U_{10} was assumed to be 7 m s^{-1}, and u_* and z_{0m} are obtained by iterative solution of the logarithmic wind profile and Charnock formula.

Figure 3 shows the normalized surface area of NaCl droplets as calculated using (8)–(10) and indicates a defined maximum for diameters between 1.0 and 6.4 μm. For this analysis, we assume that the size distribution generated by the flux equations [(8)–(10)] reasonably represents ambient marine particles in this size range.

If it is assumed that pure $NaNO_3$ is formed by the reaction of HNO_3 on sea salt particles, a deposition velocity for those particles then can be calculated using (3)–(6) for any wind speed. The deposition velocity for $NaNO_3$ particles for a wind speed of 7 m s^{-1} is shown in Fig. 4. This figure indicates that, for diameters between 1.0 and 6.4 μm, the deposition velocity is 0.02–0.8 cm s^{-1}, with a value of 0.2 cm s^{-1} for the diameter of maximum surface area ($d = 3.2$ μm).

The deposition velocity for HNO_3 can be calculated using the resistance analogue [(11)–(14)] with the assumption that the surface resistance is zero (i.e., $r_c = 0$):

$$r_a = \frac{1}{\kappa u_*}\left(\ln\frac{z_r}{z_0}\right), \tag{11}$$

$$r_b = \frac{1}{\kappa u_*}\left(\ln\frac{z_0}{z_{0_c}}\right), \tag{12}$$

$$\text{Re} < 0.15: \qquad z_{0_c} = 30\frac{\nu}{u_*}e^{-13.6\kappa \text{Sc}^{2/3}}, \quad \text{and} \tag{13}$$

$$\text{Re} \geq 0.15: \qquad z_{0_c} = 20 z_{0_m} e^{-7.3\text{Re}^{1/4}\text{Sc}^{1/2}}, \tag{14}$$

where z_{0_c} is the roughness length for the chemical of interest [from Joffre (1988) and Asman et al. (1994)]. From (11)–(14), the deposition velocity of HNO_3 for near-neutral stability and a wind speed of 7 m s^{-1} is 0.48 cm s^{-1}.

From these calculations one can observe that, for this scenario (i.e., $U = 7$ m s^{-1} and near-neutral stability), transfer of HNO_3 to the particle phase would lead to a reduction in the deposition velocity of N of over 50% (from 0.48 to 0.2 cm s^{-1}) leading to greater horizontal transport of N prior to deposition. In this way a larger geographic area could be affected by influx of anthropogenic N compounds. Alternatively stated, this result implies that, for the stated conditions, the atmospheric contribution to the N flux in the coastal zone would be reduced, but the flux to open waters would be increased by reaction of HNO_3 on sea spray particles.

To investigate whether this result may be generalized for varying conditions, the model described above was used to calculate deposition velocities for HNO_3 and $NaNO_3$ particles (with $d = 1.0$–6.4 μm) for a range of wind speed conditions and near-neutral stability. The results, shown in Fig. 5, indicate that at all wind speeds the deposition velocity for HNO_3 is within the envelope defined for particle $NaNO_3$ deposition. However, at low ($U_{10} < 3.5$ m s^{-1}) and high ($U_{10} > 10$ m s^{-1}) wind speeds the deposition velocity for HNO_3 is lower than that for an $NaNO_3$ particle of 3.2-μm diameter, and, for wind speeds between 3.5 and 10 m s^{-1}, transfer of HNO_3 to the surface is more rapid than it is for particle $NaNO_3$, indicating that transfer of N to the particle phase would decrease the deposition rate and hence increase horizontal transport of N prior to deposition. The source of the wind speed dependence in the ratio of HNO_3:$NaNO_3$ deposition velocities implied in Fig. 5 is principally that

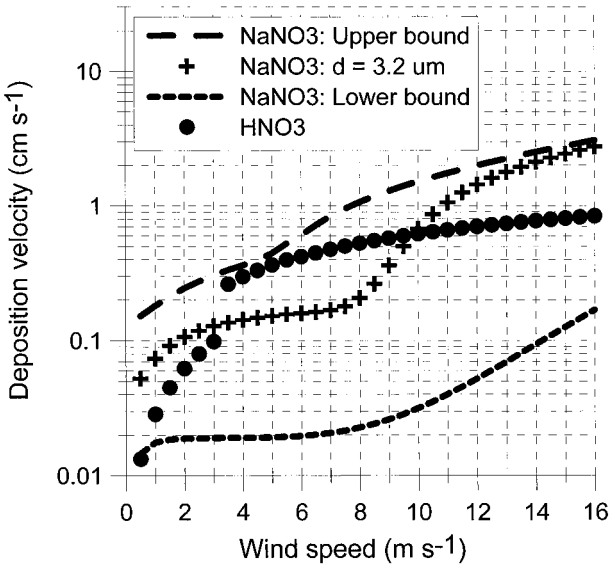

FIG. 5. Modeled particle v_d for HNO_3 and an $NaNO_3$ particle spectrum presented as a function of U_{10}. The particle spectrum was calculated from (8)–(10), and the envelope of v_d presented represents the range of v_d for particles with diameters that have a surface area equal to or greater than 60% of the maximum surface area (i.e., d = 1.0–6.4 μm). Also shown is the v_d for the diameter associated with the peak in the surface area distribution (d = 3.2 μm). As in all the simulations, u_* and z_{0m} are obtained by iterative solution of the logarithmic wind profile and Charnock formula. The step change in HNO_3 v_d at U = 3.5 m s^{-1} is due to a change in the formulas used to calculate z_{0c} [from (13)–(14)] as the Reynolds number increases above 0.15 [i.e., in the transition between smooth and rough conditions; see discussion in Joffre (1988)].

the increase of particle deposition with wind speed is greater than that of HNO_3. Particle deposition to water surfaces commonly is limited by the rate of transfer across the quasi-laminar surface layer. Resistance to this transfer is dependent on white cap activity [(6)]. As wind speed increases, white cap activity increases to the 3.75 power [(7)], and hence particle transfer across the quasi-laminar surface layer increases in a nonlinear fashion, leading to larger deposition velocities. This increase in deposition velocity with wind speed continues until the point at which transfer of particles with $d \approx$ 1.0–6.4 μm across the quasi-laminar surface layer ceases to be the major limitation on deposition.

4. Discussion and implications

An examination of the importance of HNO_3–sea salt reactions on the deposition of N to marine ecosystems has been presented. Models of sea spray generation and particle- and gas-phase dry deposition were used to compare deposition velocities for HNO_3 and $NaNO_3$ formed by reaction on sea spray.

For this study, a number of a simplifying assumptions were made. The reaction of HNO_3 on sea salt was treated in a highly simplified manner. We assume that this reaction dominates HNO_3 chemistry in the marine boundary layer, that for the conditions considered here this reaction is irreversible, that chloride deficits in sea salt aerosols are principally the result of HNO_3 reaction (or at least that uptake of other acidifying gases does not limit HNO_3 uptake), and that NaCl aerosol contains substantial water (Weiss and Ewing 1999) from the relatively high relative humidity of the marine atmospheric boundary layer [Beichert and Finlayson-Pitts (1996) have demonstrated the importance of surface water in surface uptake of HNO_3]. Further, we assume that the $NaNO_3$ formed will be concentrated at the peak in the surface-area size distribution of sea spray as described by the algorithms of Monahan et al. (1986) (i.e., d = 1.0–6.4 μm). In addition, only horizontally homogeneous conditions with near-neutral stability are treated.

Within the limits imposed by these assumptions, it is demonstrated that, at low and high wind speeds ($U_{10} <$ 3.5 m s^{-1} and $U_{10} >$ 10 m s^{-1}), the deposition velocity for HNO_3 is lower than that for the ''average'' $NaNO_3$ particle generated by surface reaction with HNO_3, and hence transfer to the particle phase would lead to increased N deposition rates. For wind speeds between 3.5 and 10 m s^{-1}, however, transfer of HNO_3 to the surface is more rapid than for particle $NaNO_3$, indicating that, at these wind speeds, transfer of N to the particle phase would decrease the deposition rate and hence increase horizontal transport of N prior to deposition. This effect may lead to a larger offshore area being affected by the products of emissions of oxides of nitrogen from coastal cities.

The results presented here emphasize the importance of particle diameter in determining particle deposition. If the role of flow divergence in the coastal zone and development of internal boundary layers is neglected, these results also imply that the numerical models currently used to estimate N deposition to the coastal zone that do not treat explicitly the HNO_3–sea spray reactions *may* overestimate the N flux under moderate wind speeds and underestimate the N flux under high wind speed conditions. Production of sea spray increases with wind speed, hence, assuming HNO_3–sea spray reaction is not limited kinetically, high wind speeds would lead to enhanced transfer of HNO_3 from the gas phase and increased deposition of N close to the source of HNO_3.

Acknowledgments. The authors acknowledge discussions with Rebecca Barthelmie and Søren Larsen of Risø National Laboratory and Michael Schulz of the University of Hamburg. This research received funding from the EU project ''BASYS,'' the Danish Research Council, Environment Canada (KE501-8-0722EDM) and NSF (ATM 971755). The authors also express thanks to the three reviewers for their comments and constructive criticisms.

REFERENCES

Asman, W. A. H., 1994: Estimation of the net air–sea flux of ammonia over the southern bight of the North Sea. *Atmos. Environ.,* **28,** 3647–3654.

——, and Coauthors, 1995: Atmospheric nitrogen input to the Kattegat. *Ophelia,* **42,** 5–28.

Barrie, L. A., J. W. Bottenheim, R. C. Schnell, P. J. Crutzen, and R. A. Rasmussen, 1988: Ozone destruction and photochemical reactions at polar sunrise in the lower Arctic atmosphere. *Nature,* **334,** 138–141.

Beichert, P., and B. J. Finlayson-Pitts, 1996: Knudsen cell studies of the uptakes of gaseous HNO3 and other oxides of nitrogen on solid NaCl: The role of surface-adsorbed water. *J. Phys. Chem.,* **100,** 15 218–15 228.

Fenter, F. F., F. Caloz, and M. J. Rossi, 1994: Kinetics of nitric acid uptake by salt. *J. Phys. Chem.,* **98,** 9801–9810.

Fisher, D., and M. Oppenheimer, 1991: Atmospheric nitrogen deposition and the Chesapeake Bay estuary. *Ambio,* **20,** 102–108.

Fitzgerald, J. W., 1975: Approximation formulas for the equilibrium size of an aerosol particle as a function of its dry size and composition and the ambient relative humidity. *J. Appl. Meteor.,* **14,** 1044–1049.

Galloway, J., H. Levy, and P. Kasibhatla, 1994: Year 2020: Consequences of population growth and development on deposition of oxidized nitrogen. *Ambio,* **23,** 120–123.

Geernaert, L. L. S., G. L. Geernaert, K. Granby, and W. A. H. Asman, 1998: Fluxes of soluble gases in the marine atmosphere surface layer. *Tellus,* **50B,** 111–127.

Hummelshøj, P., N. O. Jensen, and S. E. Larsen, 1992: Particle dry deposition to a sea surface. *Fifth Int. Conf. on Precipitation Scavenging and Atmosphere–Surface Exchange Processes,* S. E. Schwartz and W. G. N. Slinn, Eds., Hemisphere, 829–840.

Joffre, S. M., 1988: Modelling the dry deposition velocity of highly soluble gases to the sea surface. *Atmos. Environ.,* **22,** 1137–1146.

Kramm, G., and R. Dlugi, 1994: Modelling the vertical fluxes of nitric acid, ammonia and ammonium nitrate. *J. Atmos. Chem.,* **18,** 319–357.

Larsen, S. E., J. B. Edson, P. Hummelshøj, N. O. Jensen, G. de Leeuw, and P. G. Mestayer, 1995: Dry deposition of particles to ocean surfaces. *Ophelia,* **42,** 193–204.

Mamane, Y., and J. Gottlieb, 1992: Nitrate formation on sea-salt and mineral particles—A single particle approach. *Atmos. Environ.,* **26A,** 1763–1769.

Monahan, E. C., D. E. Spiel, and K. L. Davidson, 1986: A model of marine aerosol generation via whitecaps and wave disruption. *Oceanic Whitecaps,* E. C. Monahan and G. Mac Niocaill, Eds., D. Reidel, 167–174.

Paerl, H. W., 1995: Coastal eutrophication in relation to atmospheric nitrogen deposition: Current perspectives. *Ophelia,* **41,** 237–259.

Pryor, S. C., and R. J. Barthelmie, 2000: Particle dry deposition to water surfaces: Processes and consequences. *Seas at the Millennium,* C. Sheppard, Ed., Vol. 3, Elsevier Science, 127–139.

——, ——, L. L. S. Geernaert, T. Ellermann, and K. D. Perry, 1999a: Speciated particle dry deposition to the sea surface: Results from ASEPS '97. *Atmos. Environ.,* **33,** 2045–2058.

——, ——, and B. Jensen, 1999b: Nitrogen dry deposition at an AmeriFlux site in a hardwood forest in the Midwest. *Geophys. Res. Lett.,* **26,** 691–694.

Rendell, A. R., C. J. Ottley, T. D. Jickells, and R. M. Harrison, 1993: The atmospheric input of nitrogen species to the North Sea. *Tellus,* **45B,** 53–63.

Sander, R., and P. J. Crutzen, 1996: Model study indicating halogen activation and ozone destruction in polluted air masses transported to the sea. *J. Geophys. Res.,* **101,** 9121–9138.

Seinfeld, J., and S. Pandis, 1998: *Atmospheric Chemistry and Physics: From Air Pollution to Climate Change.* Wiley–Interscience, 1326 pp.

Sievering, H., D. Burton, and N. Caine, 1992: Atmospheric loadings of nitrogen to alpine tundra in the Colorado front range. *Global Biogeochem. Cycles,* **6,** 339–346.

Slinn, W., and Coauthors, 1978: Some aspects of the transfer of atmospheric trace constituents past the air–sea interface. *Atmos. Environ.,* **12,** 2055–2087.

Smith, M. H., P. M. Park, and I. E. Consterdine, 1993: Marine aerosol concentrations and estimated fluxes over the sea. *Quart. J. Roy. Meteor. Soc.,* **119,** 809–824.

Vitousek, P. M., J. D. Aber, R. W. Howarth, G. E. Likens, P. A. Matson, D. W. Schindler, W. H. Schlesinger, and D. G. Tilman, 1997: Human alteration of the global nitrogen cycle: Sources and consequences. *Eco. Appl.,* **7,** 737–750.

Weiss, D. D., and G. E. Ewing, 1999: Water content and morphology of sodium chloride aerosol particles. *J. Geophys. Res.,* **104,** 21 275–21 285.

Williams, R. M., 1982: A model for the dry deposition of particles to natural surface waters. *Atmos. Environ.,* **16,** 1933–1938.

Wu, J., 1988: Variations of whitecap coverage with wind stress and water temperature. *J. Phys. Oceanogr.,* **18,** 1488–1453.

Zufall, M. J., and C. I. Davidson, 1998: Dry deposition of particles. *Atmospheric Particles,* R. M. Harrison and R. E. van Grieken, Eds., John Wiley and Sons, 425–473.